segments, such as optically active transitions in chromophoric segments of chiral molecules.[22] Our results accord with the view[2] that a segment has no identity outside of its identity as a part of the molecule and that the symmetry of such a segment is inseparable from that of its environment.

Acknowledgment. We thank the National Science Foundation (CHE-8009670) for support of this work and J. Siegel for helpful discussions. One of us (J.E.J.) thanks Princeton University for the award of a Charlotte Elizabeth Procter Fellowship.

Registry No. Ethane, 74-84-0; 1,1,1-trifluoroethane, 420-46-2.

(22) Mason, S. F. "Molecular Optical Activity and the Chiral Discriminations"; Cambridge University Press: Cambridge, 1982.

Molybdenum(VI)–Dioxo, Molybdenum(V)–Oxo, and Molybdenum(IV)–Oxo Complexes with 2,3:8,9-Dibenzo-1,4,7,10-tetrathiadecane. Models for the Molybdenum Binding Site of the Molybdenum Cofactor

Bharat B. Kaul,[1a] John H. Enemark,[1b] Shannath L. Merbs,[1b] and J. T. Spence*[1a]

Contribution from the Department of Chemistry and Biochemistry, Utah State University, Logan, Utah 84322, and the Department of Chemistry, University of Arizona, Tucson, Arizona 85721.
Received October 22, 1984

Abstract: As possible models for the coordination of molybdenum by an unsaturated thiolate–thioether ligand in the molybdenum–pterin cofactor of molybdenum enzymes, MoO_2(dttd), MoOCl(dttd), and MoO(PPh_2Et)(dttd) ($dttdH_2$ = 2,3:8,9-dibenzo-1,4,7,10-tetrathiadecane) have been synthesized. The structure of MoO_2(dttd) has been determined by X-ray crystallography. The compound crystallizes in space group $P2_1/c$, with a = 14.34 (2) Å, b = 8.168 (6) Å, c = 14.507 (8) Å, β = 103.42 (8)°, and Z = 4. MoO_2(dttd) is six-coordinate with substantial distortion from octahedral geometry. The two thiolate S atoms are trans to one another (Mo–S_{av} = 2.402 (7) Å) and cis to the terminal oxo groups. The thioether S atoms are approximately trans to the terminal oxo groups and exhibit much longer Mo–S distances (2.687 (6) Å). MoO_2(dttd) undergoes a one-electron reversible reduction on the cyclic voltammogram time scale, but is reduced irreversibly in the presence of Et_4NCl in a two-electron step to $[MoOCl(dttd)]^-$ on the coulometric time scale; $[MoOCl(dttd)]^-$ in turn is reversibly oxidized to the EPR active monomer MoOCl(dttd). MoOCl(dttd) undergoes a reversible one-electron reduction to $[MoOCl(dttd)]^-$, but cannot be oxidized to MoO_2(dttd) in the voltage range used. MoO(PPh_2Et)(dttd) appears to lose the PPh_2Et group in DMF/Et_4NCl solution, exhibiting electrochemical behavior identical with that of $[MoOCl(dttd)]^-$. Reaction of MoO_2(dttd) with 1 equiv of PPh_2Et in DMF in the presence of Et_4NCl gives $[MoOCl(dttd)]^-$, while subsequent addition of Me_2SO to the solution regenerates MoO_2(dttd). The dimer, $Mo_2O_3(dttd)_2$, has also been obtained. It is reversibly reduced in a 1.00 electron/Mo process to $[MoOCl(dttd)]^-$ and reversibly oxidized in a 0.50 electron/Mo process to a mixture of equal amounts of MoO_2(dttd) and MoOCl(dttd) in DMF in the presence of Et_4NCl. The EPR parameters of MoOCl(dttd) and the electrochemical parameters of the various complexes are reported.

Molybdenum is an essential component of a number of enzymes that catalyze two-electron redox processes.[2,3] These enzymes have a common cofactor,[4,5] a small molybdenum-containing molecule that can be released by acid treatment of one enzyme and added to a second apoenzyme to give an active species. Recent work has identified a novel reduced pterin with a sulfur side chain from the cofactor[6] and has led to a proposed structure of the cofactor with molybdenum bound to the side chain:

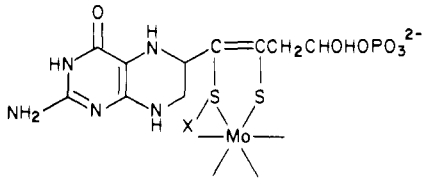

X = Me if present

Recent electronic and CD spectroscopic studies of the molybdenum domain of sulfite oxidase suggest the presence of an unusual Mo–sulfur ligand, giving some support to this structure.[7] If X = Me, the molybdenum is coordinated by an α,β-unsaturated β-mercapto thioether, a ligand type not previously reported for Mo(VI)–dioxo or Mo(V)– and (IV)–oxo complexes. Furthermore, EXAFS results have indicated two or three thiolate groups and possibly a thioether are present as ligands on molybdenum in sulfite oxidase.[8] Only two Mo(VI)–dioxo complexes and no Mo(V)– or Mo(IV)–oxo complexes with thioether coordination have been previously reported; the determination of bond lengths, electrochemical properties, and EPR parameters for such complexes is therefore of considerable interest with respect to thioether coordination in Mo enzymes.

We report here the synthesis and properties of oxomolybdenum(VI), -(V), and -(IV) complexes of 2,3:8,9-dibenzo-1,4,7,10-tetrathiadecane ($dttdH_2$), an S_4 tetradentate ligand

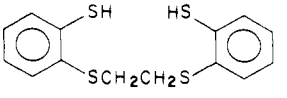

$dttdH_2$

with aromatic thiolate–thioether groups.[9] This is the first use

(1) (a) Utah State University. (b) University of Arizona.
(2) Bray, R. C. *Adv. Enzymol. Relat. Areas Mol. Biol.* **1980**, *51*, 107.
(3) Hewitt, E. J.; Notton, B. A. In "Molybdenum and Molybdenum Containing Enzymes"; Coughlan, M., Ed.; Peramon Press: New York, 1980; p 273. Ljungdahl, L. G. *Ibid.* p 463.
(4) Wahl, R. C.; Rajaopalan, K. V. *J. Biol. Chem.* **1982**, *257*, 1354.
(5) Johnson, J. L. In "Molybdenum and Molybdenum Containing Enzymes"; Coughlan, M., Ed.; Pergamon Press: New York, 1980; p 347.
(6) Johnson, J. L.; Rajagopalan, K. V. *Proc. Natl. Acad. Sci. U.S.A.* **1982**, *79*, 6856.
(7) Garner, C. D.; Buchanan, I.; Collison, D.; Mabbs, F. E.; Porter, T. G.; Wynn, C. H. In "Proceedings of the 4th International Conference on the Chemistry and Uses of Molybdenum"; Barry, H. F., Mitchell, P. C. H., Eds.; Climax Molybdenum: Ann Arbor, 1982; p 163.
(8) Cramer, S. P.; Wahl, R.; Rajagopalan, K. V. *J. Am. Chem. Soc.* **1981**, *103*, 7721.

0002-7863/85/1507-2885$01.50/0

Table I. Electrochemical Parameters

complex	E_{pc}, V[a]	E_{pa}, V[b]	E, V[c]	i_{pa}/i_{pc}[d]	$[i_p v^{-1/2} C^{-1}/(i_p v^{-1/2} C^{-1})F]$[e]	n
MoO_2(dttd)	−0.850	−0.780	0.070	0.95	0.76	1.35[f]
MoOCl(dttd)	−0.215	−0.145	0.070	0.98	0.91	0.87[f]
MoO(PPh_2Et)-(dttd)	−0.215	−0.145	0.070	1.00	0.88	1.00[g]
Mo_2O_3(dttd)$_2$	−0.880	−0.785	0.095	0.93	0.67	1.05[f]
	−0.215	−0.145	0.070	0.90	0.38	0.53[g]

[a] CV, reduction peak. [b] CV, oxidation peak. [c] $E_{pa} - E_{pc}$. [d] Peak current ratio. [e] Current function ratio, complex/ferrocene (F). [f] e^-/Mo, coulometric reduction. [g] e^-/Mo, coulometric oxidation. DMF, 0.10 M Et_4NCl, room temperature.

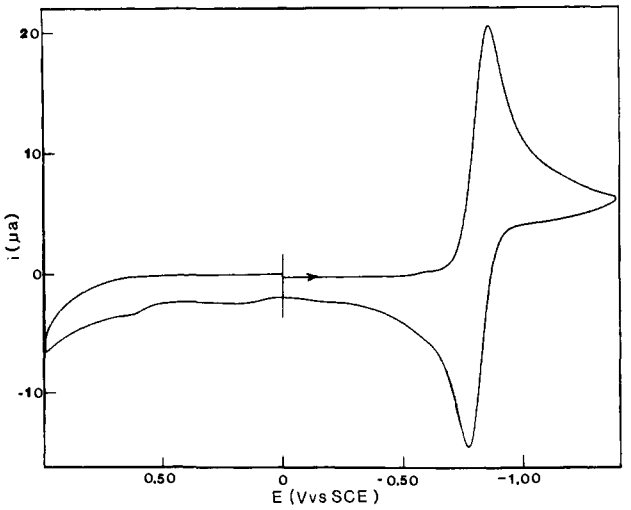

Figure 1. Cyclic voltammogram of MoO_2(dttd), 5.0×10^{-4} M. 0.10 M Et_4NCl, DMF. Scan rate = 0.100 V s^{-1}.

of such a ligand to model the molybdenum binding site of the molybdenum cofactor, although molybdenum(IV) complexes of the type MoX_2(dttd) and MoX(dttd), in which X = Cl^-, EtS^-, $C_6H_4S_2^{2-}$, and $SCH_2CH_2S^{2-}$, have been reported previously.[10]

Results

MoO_2(dttd). Reaction of $[(n\text{-}Bu)_4N]_4[Mo_8O_{26}]$ with $dttdH_2$ in MeOH gives a mixture of MoO_2(dttd) and Mo_2O_3(dttd)$_2$. MoO_2(dttd) was obtained by oxidation of the mixture with tert-butyl hydroperoxide. The complex is orange-red, with broad absorbance in the range 360–480 nm and a peak at 410 nm. The cyclic voltammogram (CV) in DMF in the presence of Et_4NCl exhibits a single reduction process centered at −0.815 V vs. SCE with ΔE_p = 0.070 V (Figure 1, Table I). No variation in ΔE was observed at scan rates up to 0.500 V s^{-1}, and i_{pa}/i_{pc} = 0.95, indicating the reduction is almost reversible for a one-electron process. The current function ($i_{pv}^{-1/2}C^{-1}$) ratio for the reduction of MoO_2(dttd) and the one-electron oxidation of ferrocene under identical conditions is 0.780, and the differential pulse polarogram (DPP) for the MoO_2(dttd) reduction has a width at half-height ($W_{1/2}$) of 0.097 V (the limiting value of $W_{1/2}$ for a one-electron reversible process as pulse amplitude approaches zero is 0.0904 V[11]), consistent with a one-electron reduction process. Coulometric reduction at −1.00 V ceases after the addition of ~1.35 electrons/molecule, giving a yellow-green, EPR silent, solution. The CV of the reduced solution exhibits a new, reversible (for one electron) oxidation process centered at −0.180 V and is identical with the CV obtained from MoO(PPh_2Et)(dttd) (vide infra), with complete loss of the redox process at −0.815 V. The height of the oxidation peak at −0.150 V is ~65% of the height of the original reduction peak at −0.815 V. Reoxidation at −0.100 V gives a deep green, EPR-active solution, with a reversible reduction process at the same potential (−0.180 V). Quantitative measurement of spin concentration indicates 65 ± 5% of total Mo is present as Mo(V) in the reoxidized solution. The EPR signal is identical with that obtained from MoOCl(dttd) (vide infra).

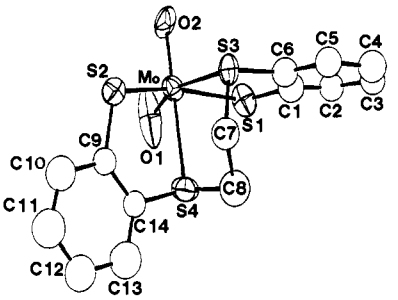

Figure 2. View of MoO_2(dttd). Hydrogen atoms omitted for clarity.

Table II. Selected Bond Distances[a] and Bond Angles

atom 1	atom 2	distance, Å	atom 1	atom 2	atom 3	angle, deg
Mo	S1	2.393 (7)	S1	Mo	S2	156.2 (3)
Mo	S2	2.411 (7)	S1	Mo	S3	79.1 (2)
Mo	S3	2.690 (6)	S1	Mo	S4	83.8 (2)
Mo	S4	2.684 (7)	S1	Mo	O1	90.0 (6)
Mo	O1	1.72 (2)	S1	Mo	O2	104.1 (5)
Mo	O2	1.71 (2)	S2	Mo	S3	81.0 (2)
			S2	Mo	S4	79.4 (2)
			S2	Mo	O1	105.1 (6)
			S2	Mo	O2	87.8 (5)
			S3	Mo	S4	78.1 (2)
			S3	Mo	O1	161.1 (1)
			S3	Mo	O2	87.1 (5)
			S4	Mo	O1	85.1 (1)
			S4	Mo	O2	161.8 (5)
			O1	Mo	O2	111.1 (1)

[a] Numbers in parentheses are estimated standard deviations in the least significant digits.

The X-ray structure of MoO_2(dttd) indicates the molecule adopts distorted octahedral geometry with the thioether atoms trans to the terminal oxo groups (Figure 2). The structure is typical of MoO_2L complexes, where L^{2-} is a linear tetradentate ligand, in this case containing four S donor atoms. The internal chelate ring angles of S1–Mo–S3, S2–Mo–S4, and S3–Mo–S4, 79.1 (2)°, 79.4 (2)°, and 78.1 (2)°, respectively, are all larger than the corresponding compound with NH groups replacing S3 and S4 [77.5 (1)°, 77.5 (1)°, 74.7 (1)°],[12] as is expected for the larger S atoms. The Mo–S1 and Mo–S2 (thiolate) distances of 2.393 (6) Å and 2.411 (7) Å are slightly shorter than the corresponding Mo–S (thiolate) distances in the above-mentioned compound of 2.429 (2e) and 2.426 (2) Å. The Mo–S3 and Mo–S4 (thioether) distances trans to the oxo groups [2.690 (6) Å, 2.684 (7) Å] are comparable to the Mo–thioether distance in the MoO_2(SSNS) compound [2.708 (1) Å][12] but are significantly shorter than the Mo–thioether distance (2.77 Å) in the tripodal complex $MoO_2[(SCH_2CH_2)_2NCH_2CH_2SCH_3]$.[13] The Mo–oxo distances of 1.72 and 1.71 Å and the O1–Mo–O2 angle of 111° also fall in the ranges that are characteristic of $MoO_2(N_2S_2)$ and MoO_2(SSNS) complexes. The molecule has effective C_2 symmetry, with the 2-fold axis bisecting the O1–Mo–O2 angle and the S3–Mo–S4 angle. The dihedral angle between the plane containing S1, S3, and C1 through C6 and the plane containing S2, S4, and C9 through C14 is 92.6°. The O1,Mo,O2 plane is twisted 12.5° from the S3,Mo,S4 plane. The poor quality of the

(9) A preliminary report of this work was presented at the 1st International Conference on Bioinorganic Chemistry, Florence, Italy, June, 1983; Subramanian, P.; Kaul, B.; Spence, J. T. *J. Mol. Catal.* **1984**, *23*, 163.

(10) Kaul, B. B.; Sellman, D. *Z. Naturforsch., B* **1983**, *38B*, 562.

(11) Bard, A. J.; Faulkner, L. R. "Electrochemical Methods. Fundamentals and Applications"; Wiley: New York, 1980; p 195.

(12) Bruce, A.; Corbin, J. L.; Dahlstrom, P. L.; Hyde, J. R.; Minelli, M.; Stiefel, E. I.; Spence, J. T.; Zubieta, J. *Inorg. Chem.* **1982**, *21*, 917.

(13) Berg, J. M.; Hodson, K. O.; Cramer, S. P.; Corbin, J. L.; Elsberry, A.; Pariyadath, N.; Stiefel, E. I. *J. Am. Chem. Soc.* **1981**, *101*, 2774. Berg, J. M.; Hodgson, K. O.; Bruce, A. E.; Corbin, J. L.; Pariyadath, N.; Stiefel, E. I. *Inorg. Chim. Acta* **1984**, *90*, 25.

Table III. Summary of Crystal and Refinement Data for $MoO_2S_4C_{14}H_{12}$[a]

space group	$P2_1/c$
a, Å	14.34 (2)
b, Å	8.168 (6)
c, Å	14.507 (8)
β, deg	103.42 (8)
V, Å^3	1650 (3)
Z	4
fw, daltons	436.45
D_{calc}, g cm^{-3}	1.757
radiation, Å	Mo K (=0.71073)
μ, cm^{-1}	12.6
scan type	ω (Wyckoff)
scan speed, deg min^{-1}	10.0
scan range, deg	1.0
bkgd counting time	0.25 times scan time
2θ limits, deg	0.0–45.0
unique reflections	2347
unique data used	866 with $\|F_o\| > 3\ \sigma(F_o)$
R	0.107
R_w	0.126
GOF	2.367

[a] GOF = $|\sum w(|F_o| - |F_c|)^2/(NO - NV)|^{1/2}$

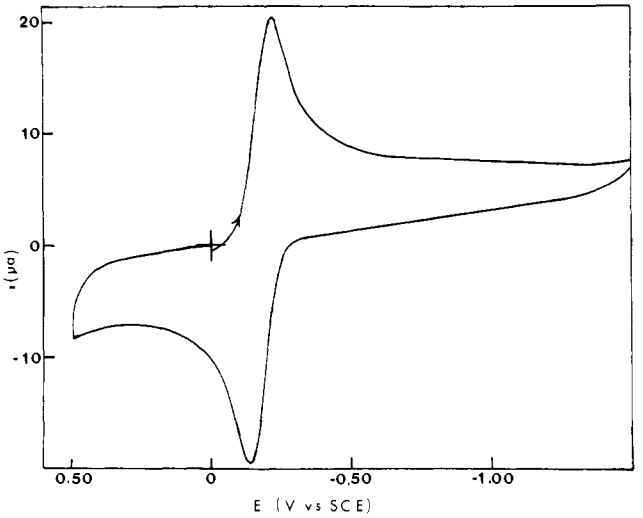

Figure 3. Cyclic voltammogram of MoOCl(dttd), 5.00×10^{-4} M. 0.10 M Et_4NCl, DMF. Scan rate = 0.100 V s^{-1}.

crystal and the necessity to collect data by the Wyckoff technique account for the high R and R_w values and the relatively large standard deviations for interatomic distances and angles (Table II and III).

The reaction between MoO_2(dttd) and [MoOCl(dttd)]$^-$ to give dimer is slow, in contrast to most Mo–oxo complexes.[14] No evidence for the presence of the dimer as an intermediate in the coulometric reduction of MoO_2(dttd) in dry solvents could be obtained, and equimolar mixtures of MoO_2(dttd) and MoO(PPh_2Et)(dttd) ($<10^{-3}$ M) in DMF in the presence of Et_4NCl develop the green color of the dimer only after standing for several hours. The reaction, however, is catalyzed by H_2O. Addition of ~0.05 mL of H_2O to 75.0 mL of a 5.00×10^{-4} M mixture of the Mo(VI) and Mo(IV) complexes results in immediate formation of the deep green color of the dimer.

Addition of 1 equiv of PPh_2Et to a 5.00×10^{-4} M solution of MoO_2(dttd) in dry DMF/0.10 M Et_4NCl results in slow (~1 h) conversion to [MoOCl(dttd)]$^-$, as determined by the CV. Subsequent addition of one drop (0.05 mL) of Me_2SO to the solution (70.0 mL) results in rapid (<1 min) regeneration of MoO_2(dttd).

MoOCl(dttd). Reaction of $(NH_4)_2MoOCl_5$ with $dttdH_2$ in dry $MeOH/CH_2Cl_2$ gives the emerald green Mo(V) monomer MoOCl(dttd). The CV of this complex in DMF exhibits a reduction process centered at –0.180 V with $\Delta E_p = 0.070$ V, identical with the CV of the two-electron reduced product of MoO_2(dttd) and the one-electron reoxidized product of the latter (Figure 3, Table I). The ratio i_{pa}/i_{pc} for the reduction is 0.98, and the current function ratio for reduction of the complex and oxidation of ferrocene is 0.91, consistent with a nearly reversible one-electron process. Coulometric reduction at –0.250 V in DMF in the presence of Et_4NCl consumed 0.87 electron/molecule of complex, giving a solution with a CV (oxidation) centered at –0.180 V and electronic spectrum identical with those obtained by the two-electron reduction of MoO_2(dttd) and from a solution of MoO(PPh_2Et)(dttd) (vide infra). In the accessible voltage range (+1.00 to –2.00 V vs. SCE) no oxidation process for MoOCl(dttd) was observed; because of limited solubility, electrochemical data in MeCN could not be obtained.

In the presence of [n-Bu_4N][BF_4] as electrolyte, the reduction occurs at the same potential, but the height of the oxidation peak at –0.145 V is much smaller than the reduction peak, and a second irreversible oxidation peak is observed at 0.390 V. Upon addition of 5.00×10^{-3} M Et_4NCl, the i_{pa}/i_{pc} ratio is restored to 0.95 and the second irreversible oxidation peak disappears. Variation of the concentration of Et_4NL over the range 5.00×10^{-3}–1.00×10^{-1} M produces no observable change in $E_{1/2}$ for the reduction.

The EPR spectrum of MoOCl(dttd) at 77 K exhibits slight rhombic distortion from axial symmetry. The g values are high and the A values relatively low, as expected for S_4 coordination (Figure 4, Table IV).

Table IV. EPR Parameters for MoOCl(dttd)[a]

g_1	g_2	g_3	$\langle g \rangle$[b]	A_1	A_2	A_3	$\langle A \rangle$[b]
2.011	1.960	1.955	1.974	6.0	1.6	4.0	3.9

[a] ^{95,97}Mo; DMF, 0.10 M Et_4NCl. A in mT. g values and $\langle A \rangle$, A_1, A_2 (or A_3) values obtained from spectra, A_3 (or A_2) calculated from $\langle g \rangle \langle A \rangle = 1/3(g_1A_1 + g_2A_2 + g_3A_3)$. [b] $\langle g \rangle$, $\langle A \rangle$, room temperature, all other values 77 K.

Table V. Electronic[a] and IR[b] Spectroscopic Data

complex	max, nm	log ϵ	ν (Mo=O), ν (Mo–O–Mo), cm^{-1}
MoO_2(dttd)	410	3.72	913 (vs), 890 (vs)[c]
MoOCl(dttd)	655	3.65	938 (vs)
	445	sh[c]	
	392	3.69	
MoO(PPh_2Et)(dttd)	595	3.15	942 (vs)
	410	3.56	
Mo_2O_3(dttd)$_2$	595	4.10	930 (vs), 755 (sh)
	398	4.05	

[a] DMF. [b] KBr disks. [c] vs = very strong, sh = shoulder.

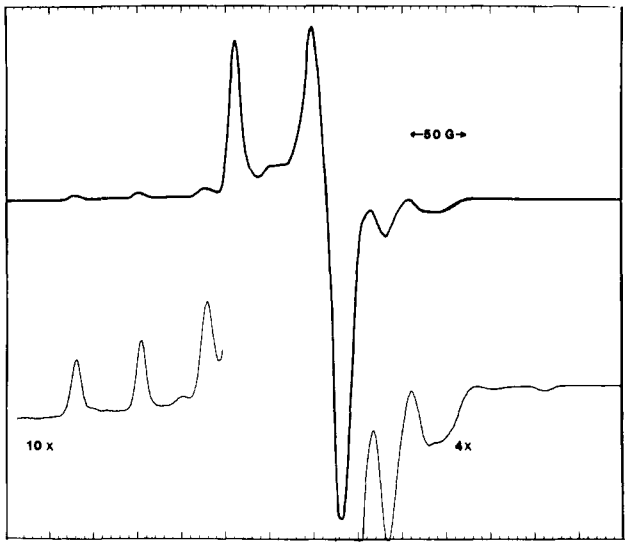

Figure 4. EPR spectrum of MoOCl(dttd), 5.00×10^{-4} M in DMF. 0.10 M Et_4NCl, 77 K.

(14) Chen, G. J.-J.; McDonald, J. W.; Newton, W. E. *Inorg. Chem.* **1976**, *15*, 2612.

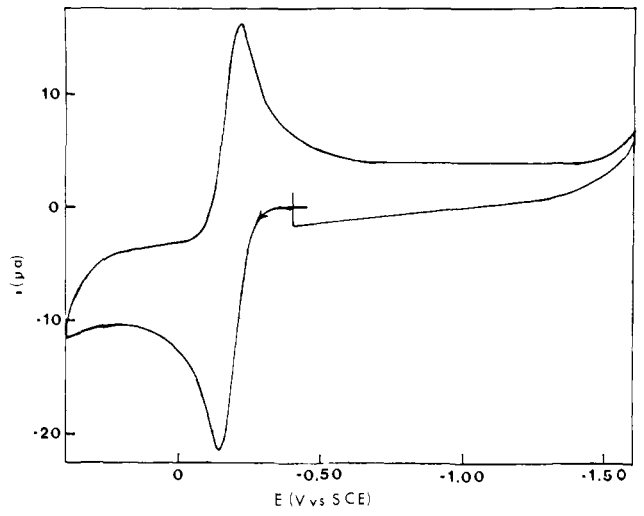

Figure 5. Cyclic voltammogram of $MoO(PPh_2Et)(dttd)$, 5.00×10^{-4} M. 0.10 M Et_4Cl, DMF.

$MoO(PPh_2Et)(dttd)$. Reduction of $MoO_2(dttd)$ with excess PPh_2Et in CH_2Cl_2 gives the yellow-green Mo(IV) monomer, $MoO(Ph_2Et)(dttd)$. The CV and electronic spectrum of this complex in DMF with Et_4NCl as supporting electrolyte are identical with those obtained from the two-electron reduction product of $MoO_2(dttd)$ and the one-electron reduction product of MoOCl(dttd) (Figure 5, Table I). Coulometric oxidation of $MoO(PPh_2Et)(dttd)$ at −0.140 V removes 1.00 electron/molecule and gives a solution with EPR and electronic spectra and CV identical with those of MoOCl(dttd).

In the presence of $[n\text{-}Bu_4N][BF_4]$ as electrolyte, the CV exhibits only several small irreversible peaks which disappear with time, accompanied by loss of the original color. It appears $MoO(PPh_2Et)(dttd)$ is unstable in DMF in the absence of excess Cl^-.

$Mo_2O_3(dttd)_2$. The Mo(V)–oxo-bridged dimer, $Mo_2O_3(dttd)_2$, was obtained by reaction of $^1/_2$ equiv of PPh_3 with $MoO_2(dttd)$:

$$2MoO_2(dttd) + PPh_3 \rightarrow Mo_2O_3(dttd)_2 + OPPh_3$$

The complex is dark green with broad absorbance in the range 550–700 nm and a peak at 595 nm. Its CV in DMF with Et_4NCl as supporting electrolyte exhibits both a reversible (for one electron) reduction at −0.835 V and a reversible oxidation at −0.180 V (Figure 6, Table I). The height of the oxidation peak is ~50% of the height of the reduction peak. Controlled potential reduction at −1.00 V consumes ~2.00 electron/molecule (1.00 electron/Mo) and gives a yellow-green solution with electronic spectrum and CV identical with those obtained by two-electron reduction of $MoO_2(dttd)$ and one-electron reduction of MoOCl(dttd) and a solution of $MoO(PPh_2Et)(dttd)$. Oxidation at −0.100 V removes ~1.00 electron/molecule (0.50 electron/Mo) and gives a deep green solution with a 50 ± 5% EPR active Mo(V) species having the same EPR spectrum as that obtained from MoOCl(dttd). The electronic spectrum of the oxidized solution indicates the presence of both $MoO_2(dttd)$ and MoOCl(dttd), and the CV is similar to that of the original $Mo_2O_3(dttd)_2$ solution except the reduction peak −0.835 V has shifted to −0.815 V and its height is almost the same as for the reduction at −0.180 V.

Discussion

Electrochemistry. The electrochemical data for $MoO_2(dttd)$ indicate the reduction centered at −0.815 V in the CV is a nearly reversible, one-electron process. On the coulometric time scale, however, the reduction clearly proceeds to the Mo(IV) complex. Furthermore, no EPR evidence could be obtained for a Mo(V) intermediate by stopping the reduction after addition of one electron/molecule, even at 0 °C, indicating that the initial one-electron reduced product rapidly undergoes further reduction with loss of an oxo group. A similar, unstable, one-electron-reduced product has been detected by EPR in the electrochemical reduction of $MoO_2(SCH_2CH_2NMe(CH_2)_2NMeCH_2CH_2S)$,[15] which also exhibits a nearly reversible CV reduction. The Mo(IV) complex, on the other hand, undergoes a nearly reversible one-electron oxidation to MoOCl(dttd) in the presence of Et_4NCl at −0.180 V on both CV and coulometric time scales. Since $MoO(PPh_2Et)(dttd)$ appears to be unstable in the absence of Cl^- and $E_{1/2}$ (reversible) for the reduction of MoOCl(dttd) does not vary with Cl^- concentration, the Mo(IV) complex is formulated as $[MoO(dttd)Cl]^-$ in the presence of excess Cl^-. These results are summarized in Scheme I. Since both $MoO_2(dttd)$ and $[MoOCl(dttd)]^-$ are relatively stable in DMF in the presence of Et_4NCl, the inability to obtain more than 1.35 electrons/molecule in the coulometric reduction of $MoO_2(dttd)$ to $[MoOCl(dttd)]^-$ (Table I) is difficult to understand. A possible cause for the low value is the instability of $MoO_2(dttd)$ in the presence of OH^-, generated in the reduction by traces of H_2O in the solvent when the oxo group is lost. Addition of 2 equiv of $[n\text{-}Bu_4N]OH$ to a solution of $MoO_2(dttd)$ in DMF (the concentration of OH^- to be expected in the complete coulometric reduction) resulted in a rapid decrease in the height of the peak, with almost complete loss over a 10-min period.

Scheme I

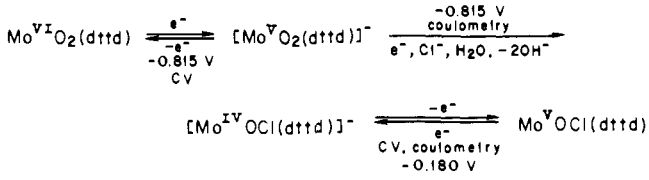

Scheme II

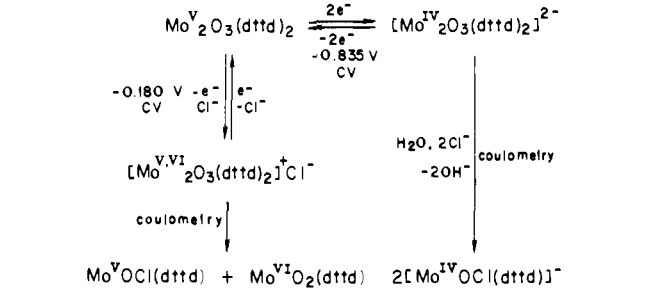

The phosphine ligand of $MoO(PPh_2Et)(dttd)$ is replaced by Cl^- in DMF solution because its CV and electronic spectrum in DMF in the presence of Et_4NCl are identical with those obtained from the two-electron reduction of $MoO_2(dttd)$ and the one-electron reduction of MoOCl(dttd). This loss of a phosphine has been previously observed for other Mo(IV)–oxo complexes.[16]

The electrochemistry of $Mo_2O_3(dttd)_2$ is unusual. The electrochemical parameters ΔE_p and i_{pc}/i_{pa} suggest the reduction at −0.835 V and the oxidation at −0.180 V in the CV are both nearly reversible one-electron processes. The low values of the current function ratios with respect to ferrocene indicate the diffusion coefficient for the dimer may differ considerably from that for ferrocene or that the processes are irreversible. The relative height of the peaks, however, indicates the reduction involves twice as many e^-/molecule as the oxidation. This is substantiated by coulometry, which shows the reduction consumes two electrons/molecule of dimer, while the oxidation yields one electron/molecule of dimer and a complex with an EPR signal identical with that of MoOCl(dttd) and which accounts for ~50% of the total Mo. Therefore, the reduction observed by CV is concluded to be an irreversible (or quasireversible) two-electron process and the oxidation a one-electron (per dimer) process. One the coulometric time scale, the initial two-electron-reduced product loses an oxo group, producing $[MoOCl(dttd)]^-$, and the initial one-electron-oxidation product gives rise to 50% $MoO_2(dttd)$ and

(15) Pickett, C.; Kumar, S.; Vella, P. A.; Zubieta, J. *Inorg. Chem.* **1982**, *21*, 908.
(16) Rice, C. A.; Spence, J. T. *Inorg. Chem.* **1980**, *19*, 2845.

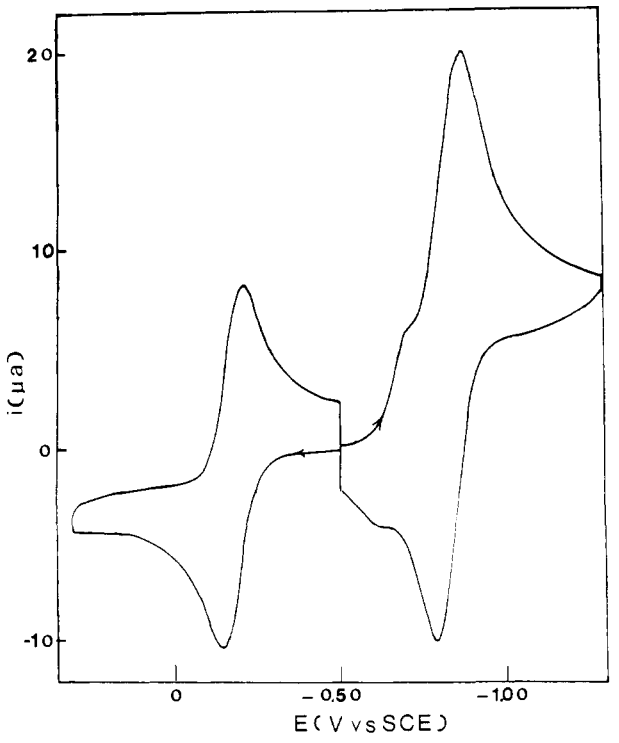

Figure 6. Cyclic voltammogram of $Mo_2O_3(dttd)_2$, 5.00×10^{-4} M. 0.10 M Et_4NCl, DMF. Scan rate = 0.100 V s^{-1}.

50% MoOCl(dttd). When $[n\text{-}Bu_4N][BF_4]$ is used as supporting electrolyte, no oxidation is observed for $Mo_2O_3(dttd)_2$ in the CV, suggesting Cl^- is involved in breaking the oxo bridge of the dimer or in stabilizing of the one-electron-oxidized product by ion-pair formation. The electrochemical results are summarized in Scheme II. It is puzzling that the oxidation potential of $Mo_2O_3(dttd)_2$ is exactly the same as the oxidation potential of $[MoOCl(dttd)]^-$, and its reduction potential is only slightly more negative (0.020 V) than that of $MoO_2(dttd)$; no obvious explanation for this suggests itself.

The above electrochemical data are the first for Mo–oxo complexes with thioether donors. It is of interest to compare the present results with data from comparable complexes with nitrogen and thiolate sulfur donors. There are two known Mo(VI)–dioxo complexes having N_2S_2 ligands of the same charge as $dttd^{2-}$ and exhibiting reversible or quasireversible reductions: $MoO_2(tox)_2$ (tox = 8-mercaptoquinoline), $E_{1/2}$ = −0.950 V,[17] and $MoO_2(SCH_2CH_2NMe(CH_2)_2NMeCH_2CH_2S)$, $E_{1/2}$ = −1.265 V.[15] $E_{1/2}$ for $MoO_2(dttd)$ (−0.815 V) is significantly more positive, indicating the thioether group is more effective than either an aliphatic or aromatic nitrogen in stabilizing the lower (Mo(V)) oxidation state. The only reported Mo(V)–oxo complex with a comparable donor set is $MoOCl(SCMe_2CH_2NHCH_2CH_2NHCH_2CMe_2S)$, $E_{1/2}$ = −0.415 V (quasireversible),[17] again indicating the thioether group of MoOCl(dttd) ($E_{1/2}$ = −0.180 V) is more effective than an aliphatic nitrogen in stabilizing the lower (Mo(IV)) oxidation state.

EPR. No EPR data for Mo(V)–oxo complexes having thioether donors have been previously reported. Since recent EXAFS results for the Mo enzyme sulfite oxidase suggest the possibility of thioether coordination of Mo,[8] the effect of such coordination on the g and A (^{95,97}Mo) values is of considerable interest. The structure of MoOCl(dttd) is unknown, but all Mo(V)–oxo complexes containing a Cl^- for which structures are known have the Cl^- cis to oxo. The thiolate groups are also cis to the oxo group and trans to each other.[18,19] If this geometry occurs for MoOCl(dttd), then the equatorial ligands (in the plane normal to the Mo=O group) are two thiolates, a Cl^- and one thioether sulfur. For MoOCl(dttd), $\langle g \rangle$ = 1.974, significantly higher than the $\langle g \rangle$ values for related Mo(V)–oxo complexes with NS_2Cl equatorial ligands (1.97–1.969)[19] which have either aliphatic or aromatic nitrogen donors. The $\langle A \rangle$ values, on the other hand, are comparable (3.85 mT vs. 3.79–3.80 mT).[19] The known $\langle g \rangle$ values for $[MoO(SPh_4)]^-$[20] (1.990) and for complexes with ligands having two thiolate sulfur and two deprotonated trigonal (amido) nitrogens (1.986–1.990)[21] suggest that the thioether group is comparable to thiolate or amido nitrogen in its effect on Mo(V) g values.

Structure of MoO_2dttd. The X-ray structure of $MoO_2(dttd)$ is comparable to the structures of Mo(VI)–dioxo complexes with tetradentate N_2S_2 ligands having five-membered rings.[12,18] The Mo–thioether sulfur bond lengths are of some interest, since aromatic thioether–Mo bond lengths have not previously been reported. They are slightly shorter than aliphatic thioether Mo bonds and significantly shorter than the possible Mo–thioether bond postulated from EXAFS results for sulfite oxidase (2.69 Å vs. 2.82–2.86 Å).[8]

Reactions of MoO_2(dttd) and MoO(dttd). Recently Berg and Holm have reported $MoO_2(LNS_2)$ (LNS_2 = pyridine-2,6-bis-(2,2-diphenylethanethiolato)) catalyzes the oxidation of PPh_3 by Me_2SO,[22] and the oxidation of tertiary phosphines by other Mo(VI)–dioxo complexes has been studied.[23,24] The present study of thiolate–thioether complexes of Mo has focused on synthesis, structure, and spectroscopic and electrochemical properties. The qualitative results concerning the reduction of $MoO_2(dttd)$ by PPh_2Et and the reoxidation of $[MoOCl(dttd)]^-$ by Me_2SO, however, suggest $MoO_2(dttd)$ will serve in a similar catalytic manner, with little, if any, dimer formation:

$$MoO_2(dttd) + PPh_2Et + Cl^- \rightarrow [MoOCl(dttd)]^- + OPPh_3Et \quad \text{slow}$$

$$[MoOCl(dttd)]^- + Me_2SO \rightarrow MoO_2(dttd) + Me_2S + Cl^- \quad \text{fast}$$

Detailed kinetic studies of these and other redox reactions of $MoO_2(dttd)$ and $[MoO(dttd)Cl]^-$ are planned and will be reported later.

Conclusion

The results indicate α,β-unsaturated β-mercaptothioether coordination of Mo results in properties consistent with, if not identical with, those of the Mo center of sulfite oxidase. The Mo–thioether sulfur bond distances in $MoO_2(dttd)$ are somewhat shorter than the possible thioether EXAFS bond length in sulfite oxidase; the EXAFS data, however, are not precisely known. The EPR parameters for MoOCl(dttd) are similar to those for sulfite oxidase[25] ($\langle g \rangle$ = 1.980, A_1 = 6.3 mT, low pH form), and the electrochemistry and reactivity of $MoO_2(dttd)$ mimic certain aspects of the redox behavior of sulfite oxidase: reversible one-electron processes on the CV time scale for the Mo(VI/V) and Mo(V/IV) couples, two-electron coulometric reduction to $[MoOCl(dttd)]^-$ without dimer formation, and chemically reversible oxo transfer reactions between substrates and $MoO_2(dttd)$ and $[MoOCl(dttd)]^-$. Thus, the proposed structure for the Mo

(17) Taylor, R. D.; Street, J. P.; Minelli, M.; Spence, J. T. *Inorg. Chem.* **1978**, *17*, 3207.
(18) Yamanouchi, K.; Enemark, J. H. *Inorg. Chem.* **1979**, *18*, 1626.
(19) Scullane, M. I.; Taylor, R. D.; Minelli, M.; Spence, J. T., Yamanouchi, K.; Enemark, J. H. *Inorg. Chem.* **1979**, *18*, 3213.
(20) Hanson, G. R.; Brunette, A. A.; McDonnell, A. E.; Murray, K. S.; Wedd, A. G. *J. Am. Chem. Soc.* **1981**, *103*, 1953.
(21) Rajan, O. A.; Spence, J. T.; Leman, C.; Minelli, M.; Sato, M.; Enemark, J. H.; Kroneck, P. M. H.; Sulger, K. *Inorg. Chem.* **1983**, *22*, 3065.
(22) Berg, J. M.; Holm, R. H. *J. Am. Chem. Soc.* **1984**, *106*, 3035; Pure Appl. *Chem.* **1984**, *56*, 1645.
(23) Toppich, J.; Lyon, J. T., III. Polyhedron **1984**, *3*, 61; *Inorg. Chim. Acta* **1983**, *80*, L41.
(24) Reynolds, M. S.; Berg, J. M.; Holm, R. H. *Inorg. Chem.* **1984**, *26*, 3057.
(25) Bray, R. C. In "Biological Magnetic Resonance"; Berliner, L. J., Reuben, J., Eds.; Plenum Press: New York 1980; Vol. 2, p 45.

binding site of the Mo–pterin cofactor should be considered as a plausible model.

Experimental Section

Materials. *o*-Aminobenzenethiol, 1,2-dibromoethane, tetra-*n*-butylammonium tetrafluoroborate, tetraethylammonium chloride, and sodium molybdate dihydrate were obtained from Aldrich Chemical Co., and triphenylphosphine (PPh_3) and diphenylethylphosphine (PPh_2Et) from Strem Chemicals, Inc.

All solvents were reagent grade, purified and dried by standard methods. $[(n\text{-}Bu)_4N]_4Mo_8O_{26}$[26] and $(NH_4)_2MoOCl_5$[27] were prepared by literature methods and $dttdH_2$ as described by Sellmann and Bohlen.[28]

MoO_2(dttd). $[(n\text{-}Bu)_4N]Mo_8O_{26}$ (1.00 g, 0.46 mmol) was dissolved in 25 mL of hot MeOH. The solution was cooled in an ice bath and 1.08 g (3.47 mmol) of $dttdH_2$, dissolved in 4 mL of CH_2Cl_2, was added dropwise with stirring over a 1-h period (if the $dttdH_2$ is added too fast, the major product is the dimer $Mo_2O_3(dttd)_2$). The color of the solution became orange and then dark green. The mixture was stirred for 4 h, and the green-brown solid was collected by filtration, washed several times with small portions of MeOH and diethyl ether, and dried in vacuo at room temperature. The solid was extracted with 40 mL of CH_2Cl_2 and the solution filtered. To the filtrate, 0.30 mL of tert-butyl hydroperoxide was added and the mixture stirred for 1.5 h, during which time the color changed to orange-red. The solution was concentrated to 7.0 mL under vacuum and orange-red crystals separated. They were filtered off, washed with MeOH and diethyl ether, and dried overnight in vacuo at room temperature. The crude product was recrystallized from CH_2Cl_2/MeOH at −20°, giving orange-red crystals (0.65 g, 70% yield). Anal. Calcd for $MoC_{14}H_{12}O_2S_4$: C, 38.53; H, 2.77; S, 29.39. Found: C, 38.52; H, 2.78; S, 29.12.

MoOCl(dttd). All operations were performed under N_2 using deaerated solvents. A solution of $dttdH_2$ (0.39 g, 1.20 mmol) in 25 mL of CH_2Cl_2 was added dropwise with stirring to 0.40 g (1.2 mmol) of $(NH_4)_2MoOCl_5$ in 10 mL of dry MeOH. The deep green solution was stirred for 2.5 h, and the white precipitate of NH_4Cl was separated by filtration and the filtrate concentrated to ~12 mL. The solution was kept overnight at −20°, during which time deep green crystals separated. The crystals were collected by filtration, washed with dry MeOH and Et_2O, and dried in vacuo at room temperature. The product was recrystallized from CH_2Cl_2/MeOH at −20 °C, giving 0.11 g (20% yield) of emerald green crystals. Anal. Calcd for $MoC_{14}H_{12}ClOS_4$: C, 36.88; H, 2.65; Cl, 7.77; S, 28.13. Found: C, 36.88; H, 2.66; Cl, 7.89; S, 27.94.

MoO(PPh_2Et)(dttd). All operations were carried out under N_2 with deaerated solvents. PPh_2Et (0.60 mL, 2.8 mmol) was added with stirring to a solution of 0.30 g (0.68 mmol) of MoO_2(dttd) in 25 mL of dry CH_2Cl_2. The mixture initially turned green. After the mixture was stirred for 4.5 h at room temperature, the color gradually changed to yellow-green. The reaction time is very important; shorter times give a mixture of the product and Mo_2O_3(dttd), while with longer times the product is contaminated with an unknown, non-oxo species. The solvent was removed to dryness under vacuum, and the resulting oily residue was triturated with 25 mL of dry Et_2O, giving a yellow-green solid. The solid was removed by filtration, washed with dry MeOH, and dried in vacuo at room temperature. The solid was recrystallized from CH_2Cl_2/MeOH at −20° to give 0.15 g (35% yield) of light green-yellow product. Anal. Calcd for $MoC_{28}H_{27}OPS_4$: C, 52.98; H, 4.28; P, 4.88; S, 20.20. Found: C, 52.80; H, 4.25; P, 4.71; S, 19.96.

Mo_2O_3(dttd)$_2$. PPh_3 (0.090 g, 0.34 mmol) in 5 mL of CH_2Cl_2 was added with stirring to a solution of 0.30 g (0.68 mmol) MoO_2(dttd) in 20 mL CH_2Cl_2. The color of the solution immediately turned dark green. Stirring was continued for ~4 h, during which time a dark green solid separated. MeOH (15 mL) was added and the dark green solid collected by filtration, washed with MeOH and diethyl ether, and dried in vacuo at room temperature. The crude product was recrystallized from CH_2Cl_2/MeOH at −20 °C, giving dark green microcrystals, yield 40%. Anal. Calcd for $Mo_2C_{28}H_{24}O_3S_8$: C, 39.25; H, 2.82; S, 29.94. Found: C, 38.96; H, 3.03; S, 29.71.

Electrochemistry. Cyclic voltammetry, differential pulse polarography (DPP), and coulometry were performed in DMF (Burdick and Jackson, dried over molecular sieves), with Et_4NCl or $[n\text{-}Bu_4N][BF_4]$ as electrolyte, using a three-electrode cell described previously[17] and a PAR Model 173 potentiostat, 174 polarographic analyzer, and 175 signal generator. Potential measurements have a precision of ±0.005 V and coulometric measurements (n) of ±10%.

Table VI. Positional Parameters and Their Estimated Standard Deviations[a]

atom	x	y	z	B_{eq}, Å^2
Mo	0.2743 (2)	0.0139 (4)	0.1846 (2)	3.23 (6)
S1	0.4411 (6)	0.084 (1)	0.2232 (6)	4.4 (3)
S2	0.1076 (6)	0.039 (1)	0.1041 (6)	4.2 (2)
S3	0.2965 (6)	0.124 (1)	0.0162 (6)	3.3 (2)
S4	0.2487 (7)	0.337 (1)	0.2002 (6)	4.4 (3)
O1	0.275 (2)	0.007 (6)	0.303 (2)	10 (1)
O2	0.272 (1)	−0.179 (3)	0.138 (1)	4.4 (6)
C1	0.484 (2)	0.150 (5)	0.124 (2)	4.6 (9)*
C2	0.577 (2)	0.176 (5)	0.133 (2)	4.1 (8)*
C3	0.614 (2)	0.241 (5)	0.057 (2)	4.1 (8)*
C4	0.555 (3)	0.258 (5)	−0.031 (2)	4.9 (9)*
C5	0.457 (2)	0.221 (5)	−0.045 (2)	4.2 (9)*
C6	0.420 (2)	0.161 (5)	0.035 (2)	4.2 (8)*
C7	0.247 (2)	0.322 (5)	0.010 (2)	4.5 (9)*
C8	0.289 (3)	0.435 (5)	0.101 (3)	6 (1)*
C9	0.066 (2)	0.235 (4)	0.128 (2)	3.3 (7)*
C10	−0.033 (3)	0.251 (5)	0.107 (2)	5.2 (9)*
C11	−0.070 (3)	0.389 (6)	0.128 (3)	6 (1)*
C12	−0.016 (2)	0.524 (5)	0.162 (2)	5.6 (9)*
C13	0.088 (2)	0.508 (6)	0.187 (2)	6 (1)*
C14	0.123 (3)	0.360 (4)	0.168 (2)	3.1 (7)*

[a] Starred atoms were refined isotropically. Anisotropically refined atoms are given in the form of the isotropic equivalent thermal parameter defined as $8\pi^2(U_{11} + U_{22} + U_{33})/3$.

EPR. EPR spectra were obtained with a Varian E-109 spectrometer. Samples were prepared under N_2, transferred to EPR tubes with gas-tight syringes, and frozen immediately in liquid N_2. Room temperature spectra were obtained with a flat cell under Ar.

EPR parameters were obtained from the measured spectra by inspection, using DPPH as standard. Spin concentrations (±10%) were estimated by using known Mo(V) complexes ($K_3Mo(CN)_8$, MoOCl(thiooxine)$_2$) as standards.

Collection and Processing of Crystallographic Data. Many crystals from several different preparations were examined under a polarizing microscope. All were of poor quality, showing many microfractures. The best crystal that could be found, measuring 0.25 × 0.2 × 0.1 mm, was mounted on the tip of a slim glass fiber with epoxy cement.

The determination of the Bravais lattice and cell dimensions and the collection of intensity data were carried out with a Syntex $P2_1$ diffractometer equipped with a graphite monochromator. The cell dimensions were based on the centering of 23 reflections with $5° < 2\theta(\text{Mo K}\alpha) < 20°$. After the least-squares refinement of the setting angles, axial photos were used to check the crystal system and axial lengths. Several ω-scans showed very broad Bragg peaks (width at half-height 1.03°), as was expected from the optical examination of the crystal. The crystal and diffractometer data are listed in Table III.

Intensity data were collected at ambient temperature with Mo Kα radiation. A Wyckoff scan technique was used because of the large mosaicity of the crystal. Backgrounds were measured 1.75° above and below the peak maximum. A quadrant of data was collected, h, $k \pm 1$ out to $2\theta = 45°$. The intensities of two standard reflections, measured every 98 reflections, showed no decay during data collection. Systematic absences in the data showed the monoclinic space group to be $P2_1/c$. Corrections were made for Lorentz and polarization effects, but no attempt was made to correct for absorption or extinction.

The structure determination and refinement were carried out with the SDP series of crystallographic programs on a PDP 11/34a computer.[29] A Patterson synthesis yielded the positions of the molybdenum atom and the four sulfur atoms. Susequent difference Fourier syntheses located the remaining nonhydrogen atoms. In the final cycles, the noncarbon atoms were refined anisotropically, and the carbon atoms were refined isotropically. Atom O1 showed large anisotropic thermal motion. This may reflect the poor quality of the data crystal, but similar behavior has been seen in related dioxomolybdenum(VI) compounds.[12] The hydrogen atoms were treated as fixed contributors ($B = 5.0$ Å^2) in idealized positions. Refinement converged to $R = 0.107$ and $R_w = 0.126$, based on the minimization of $\sum w(|F_o| - |F_c|)^2$, where $w^{-1} = \sigma^2(F_o) + 0.25(cF_o)^2$ with $c = 0.03$. The highest peak from the final difference map was 1.4

(26) Fuchs, J.; Hartl, H. *Angew Chem., Int. Ed. Engl.* **1976**, *15*, 375. Klemperer, W. G.; Shum, W. *J. Am. Chem. Soc.* **1976**, *98*, 8291.
(27) Palmer, W. G. "Experimental Inorganic Chemistry"; Cambridge University Press, Cambridge, UK, 1934; p 408.
(28) Sellman, D.; Bohlen, E. *Z. Naturforsch., B* **1982**, *37B*, 1026.
(29) Computer programs used for this analysis: (1) The Structure Determination Package (SDP) (B. A. Frenz and Associates, Inc., College Station, TX 77840 and Enraf-Nonius, Delft, Holland); (2) ORTEP 2 (Johnson, C. K. Report ORNL-3794, Oak ridge National Laboratory, Oak Ridge, TN). ORTEP 2 is included in the SDP software.

eÅ^{-3} at 1.17 Å from the molybdenum atom. The final fractional coordinates and thermal parameters of the refined atoms are listed in Table VI.

Acknowledgment. Financial support of this work by NIH Grant GM 08347 and NSF Grant CHE-8402136 (JTS) and NIH Grant ES 00966 (JHE) is gratefully acknowledged. We thank Dr. R. Ortega for assistance with the X-ray structure determination.

Supplementary Material Available: Listings of idealized hydrogen atom positions, additional bond distances and angles, thermal parameters, and structure factors for MoO_2(dttd) (9 pages). Ordering information is given on any current masthead page.

1,2-Methyl Shift between Pt and the Coordinated Aryl Group in the Reaction of Methyl Iodide with 2,6-Bis[(dimethylamino)methyl]phenyl-*N*,*N*′,*C* Complexes of Platinum(II). X-ray Crystal Structure of the Arenonium–Platinum Compound [Pt(*o*-tolyl)($MeC_6H_3(CH_2NMe_2)_2$-*o*,*o*′)]I

Jos Terheijden,[†] Gerard van Koten,*[†] Ico C. Vinke,[‡] and Anthony L. Spek[‡]

Contribution from the Anorganisch Chemisch Laboratorium, University of Amsterdam, J. H. van't Hoff Instituut, Nieuwe Achtergracht 166, 1018 WV Amsterdam, The Netherlands, and Vakgroep Algemene Chemie, Afdeling Kristal- en Struktuurchemie, University of Utrecht, 3584 CH Utrecht, The Netherlands. *Received September 10, 1984*

Abstract: The ionic complexes [PtX($MeC_6H_3(CH_2NMe_2)_2$-*o*,*o*′)]OTf (X = Cl, Br, I) prepared from the reaction of [PtX-($C_6H_3(CH_2NMe_2)_2$-*o*,*o*′)] with MeOTf possess a σ-metal-substituted arenonium ion with the Pt–C σ-bond trans to the halide. Synthetic investigations revealed that not only these species with X = Cl, Br, and I trans to the arenonium unit were isolable but also complexes with a more sterically demanding tolyl (ortho or para) group were formed in the reaction of [Pt(tolyl)($C_6H_3(CH_2NMe_2)_2$-*o*,*o*′)] with MeI. A single-crystal X-ray study has revealed the structure of the complex [Pt(*o*-tolyl)($MeC_6H_3(CH_2NMe_2)_2$-*o*,*o*′)]I (see Figure 3): triclinic, space group $P\bar{1}$ with a = 7.295 (2) Å, b = 9.832 (2) Å, c = 15.044 (3) Å, α = 87.47 (2)°, β = 86.24 (2)°, γ = 83.42 (2)°, and Z = 2. The intensities of 3481 independent reflections were used to determine the structure. The structure was solved and refined using standard heavy-atom and least-squares techniques. The approximately square-planar complex has a σ-bonded *o*-tolyl group (Pt–C = 2.005 (9) Å) twisted perpendicular to the coordination plane and trans to the σ-bonded arenonium unit with Pt–C = 2.293 (9) Å. These and other experimental findings provide new evidence regarding oxidative-addition reductive-elimination pathways. It is concluded that attack of the methylating reagent occurs at the metal center. Hereby a five-coordinate cationic Pt^{IV}–Me intermediate is formed that can consequently rearrange via two pathways, either (i) overall reductive elimination of MeX (in the case of X = Cl, Br, I) or (ii) 1,2-methyl shift across the Pt–C bond (Scheme I). Steric hindrance of the trans group and/or the presence of a nucleophile influence the available pathways which are discussed in detail.

In general organometallic complexes have been shown to be the active species in many metal-mediated organic and catalytic synthetic reactions. Extensive efforts have been made in preparing suitable organometallic compexes that, as models for reactive intermediates, can be used to study crucial steps of these processes in detail. In particular, there is a considerable interest in the oxidative addition reactions of organometallic complexes with electrophiles such as alkyl halides, halogens, or metal salts.[1-4] Detailed studies have been undertaken to improve the understanding of the mechanisms of reactions of electrophiles with group 8–10 metals[2,3,33] and of reactions involving C–C bond formation.[5-8] Evidence has been put forward that these reactions of d^8 organometallics may take place either by a direct attack of the electrophile on the carbon atom of the metal–carbon bond or by prior oxidative addition of the electrophile to the transition metal, followed by reductive elimination of the organic product.[4-6] The occurrence of the direct attack mechanism can be proved by detection of the oxidative-addition intermediate, which in a subsequent reaction provides the reductive-elimination product.[9-11] A further mechanism that has been suggested involves attack by the electrophile on the metal–carbon bond itself.[7,12]

In the course of a study of the addition of alkyl halides to the cationic complex [Pt($C_6H_3(CH_2NMe_2)_2$-*o*,*o*′)(H_2O)]BF_4 (**1**) we reported that when MeI was used, instead of the expected five-coordinate oxidative addition product [Pt(Me)I(C_6H_3-

[†] University of Amsterdam.
[‡] University of Utrecht.

(1) Johnson, M. D. *Acc. Chem. Res.* **1978**, *11*, 57.
(2) Kochi, J. K. "Organometallics Mechanisms and Catalysis"; Academic Press: New York, 1978.
(3) Appleton, T. G.; Clark, H. C.; Manzer, L. E., *J. Organomet. Chem.* **1974**, *65*, 275.
(4) van der Ploeg, A. F. M. J.; van Koten, G.; Vrieze, K.; Spek, A. L. *Inorg. Chem.* **1982**, *21*, 2014.
(5) Brown, M. P.; Puddephatt, R. J.; Upton, C. E. E. *J. Chem. Soc. Dalton Trans.* **1974**, 2457.
(6) Gillie, A.; Stille, J. K. *J. Am. Chem. Soc.* **1980**, *102*, 4933.
(7) Belluco, U.; Michelin, R. A.; Uguagliati, P.; Crociani, B. *J. Organomet. Chem.* **1983**, *250*, 565.
(8) Braterman, P. S.; Cross, R. J.; Young, G. B. *J. Chem. Soc., Dalton Trans.* **1974**, 1892.
(9) Jawad, J. K.; Puddephatt, R. J. *Inorg. Chim. Acta* **1978**, *31*, L391.
(10) Kuyper, J. *Inorg. Chem.* **1978**, *17*, 1458.
(11) van der Ploeg, A. F. M. J.; van Koten, G.; Vrieze, K. *J. Organomet. Chem.* **1982**, *226*, 93.
(12) Romeo, R.; Minniti, D.; Lanza, S.; Uguagliati, P.; Belluco, U. *Inorg. Chem.* **1978**, *17*, 2813.

0002-7863/85/1507-2891$01.50/0